ADVANCED OPTICAL MATERIALS
www.advopticalmat.de

Materials Views
www.MaterialsViews.com

Transverse Electric Mode for Near-Field Radiative Heat Transfer in Graphene–Metamaterial Systems

D. Drosdoff, A. D. Phan, and L. M. Woods**

Electromagnetic fluctuations give rise to several interesting phenomena, such as Casimir/van der Waals interactions,[1] quantum friction[2] and heat radiation.[3] Due to device miniaturization, there has been renewed interest in such effects because electromagnetic fluctuations can have a sizable and often a dominant role in micro- and nanoscale applications. Although far-field (FF) radiation is of great relevance, such as being the main source of energy on earth from the sun, when the separation between objects of different temperatures is decreased to the sub-micrometer scale, near-field (NF) radiation becomes dominant, and the heat exchange can be enhanced by several orders of magnitude. This effect is due to tunneling of evanescent electromagnetic waves, which disappear at larger distances. Because of its strong sensitivity to the material properties and its ability to greatly enhance the heat transfer, this phenomenon can be used for many applications, including thermophotovoltaics, refrigeration and thermal rectifiers.[4]

Strong NF radiation enhancement occurs in materials which are able to support surface plasmon-polaritons or phonon-polaritons in the infrared regime.[5] The main challenge has been to find ways to control these modes in order to achieve resonant coupling between the objects. Systems allowing for tunable evanescent excitations in the infrared range are desirable. Materials, such as Si, SiC, and other metals are suitable, however achieving tunability of the plasmon frequency via typical carrier density variations is problematic.[6] The discovery of graphene and its related derivatives opens up possibilities for new ways of photon tunneling management. In particular, graphene plasmons are dispersive, and they depend strongly on the chemical doping, electromagnetic gating, and temperature, which is advantageous for the radiative heat transfer.[7,8]

For most materials, the near-field radiation usually occurs through the transverse magnetic (TM) electromagnetic modes while the contribution from the transverse electric (TE) modes is negligible, as demonstrated experimentally.[9–11] Graphene has been shown to support plasmons with both polarizations,[12] but its TE plasmon is weaker and close to the photon line, which makes its relevance to radiation small.[8] We propose that under certain conditions, it is possible that the graphene TE electromagnetic modes can give a detectable contribution to the radiative heat exchange. We also suggest that this becomes available when artificial, optical metamaterials are utilized.

Optical metamaterials (MMs) are man-made composites which, unlike naturally occurring materials, have dielectric and magnetic responses in the terahertz, infrared and/or visible ranges.[13,14] It has been shown that the NF radiation between MMs can be further increased by opening both the TE and TM channel radiative modes.[15] Here we investigate the possibility of heat exchange between such a MM and graphene. The motivation comes from the fact that by a resonant electromagnetic coupling, one is able to obtain tunable heat transfer via TE and/or TM polarized modes. Our study shows that the MM/graphene system enables novel pathways for heat transfer control through the properties of graphene and the MM. In addition, basic understanding of graphene characteristics is advanced. For example, the close relationship between the TE part of the heat exchange and the relaxation rates may be used as a measuring tool for scattering processes in graphene and their temperature dependence.

The thermal radiation between two parallel, planar systems may be found from the theory of fluctuation phenomena in which electromagnetic excitations are dissipated via radiation through their response functions. The radiated power between planar objects held at temperatures T_1 and T_2 is:[3]

$$P_{NF,FF} = \int_0^\infty d\omega \hbar\omega \left[\frac{1}{e^{\hbar\omega/k_B T_2} - 1} - \frac{1}{e^{\hbar\omega/k_B T_1} - 1} \right] \sum_{i=p,s} f_i^{NF,FF}(\omega)$$

$$f_i^{NF}(\omega) = \frac{1}{\pi^2} \int_{\omega/c}^\infty dq q e^{-2\sqrt{q^2-\omega^2/c^2}\,d} \left[\frac{\Im m(\rho_{i1}) \Im m(\rho_{i2})}{|1 - \rho_{i1}\rho_{i2} e^{-2\sqrt{q^2-\omega^2/c^2}\,d}|^2} \right]$$

$$f_i^{FF}(\omega) = \frac{1}{4\pi^2} \int_0^{\omega/c} dq q \left[\frac{(1-|\rho_{i1}|^2)(1-|\rho_{i2}|^2)}{|1 - \rho_{i1}\rho_{i2} e^{-2\sqrt{q^2-\omega^2/c^2}\,d}|^2} \right], \quad (1)$$

where q is the 2D wave vector. The spectral functions $f_i(\omega)$ for the NF and FF regimes include the reflection coefficients $\rho_{i1,2}$ for the $i = s$ (TE) and $i = p$ (TM) polarizations, which contain important materials properties for the exchange process.

Equation (1) shows that the magnitude of the heat power is also dictated by the overlap of the $\Theta(\omega) = \hbar\omega / (e^{\hbar\omega/k_B T} - 1)$

Dr. D. Drosdoff, Prof. L. M. Woods
Department of Physics
University of South Florida
Tampa, FL 33620, USA
E-mail: david.drosdoff@gmail.com; lmwoods@usf.edu
A. D. Phan
Department of Physics
University of Illinois at Urbana-Champaign
61801, USA
A. D. Phan
Institute of Physics
Vietnam Academy of Science and Technology
Hanoi 1000, Vietnam

DOI: 10.1002/adom.201400275

function and the spectral function $f_i(\omega)$. The larger overlap warrants greater dissipated energy. The maximum of the Θ function is typically given by frequencies close to those given by Wien's displacement law, which at room temperature is $\hbar\omega \approx 0.1eV$. Thus the material properties must be such that the spectral function has a maximum in this range, if stronger heat transfer is desired.

The thermal radiation exchange between two identical graphene sheets is considered first. The reflection coefficients in this case are $\rho_{s1,2} = 2\pi i\sigma\omega / (\sqrt{q^2-\omega^2} - 2\pi i\sigma\omega)$ and $\rho_{p1,2} = 2\pi i\sigma\sqrt{q^2-\omega^2} / (\omega + 2\pi i\sigma\sqrt{q^2-\omega^2})$. The conductivity of each graphene, σ, is taken via a two-band tight-binding Dirac model[16]

$$\sigma_D = \frac{i}{\omega + i\Gamma}\frac{e^2 2k_B T}{\pi\hbar^2} ln\left[2\cosh\left(\mu / 2k_B T\right)\right],$$

$$\sigma_I = \frac{e^2}{4\hbar}\left[G(\hbar\omega/2) + i\frac{4\hbar\omega}{\pi}\int_0^\infty d\zeta \frac{G(\zeta) - G(\hbar\omega/2)}{(\hbar\omega)^2 - 4\zeta^2}\right], \quad (2)$$

where σ_D denotes the intra-band contributions with μ being the chemical potential and Γ- the relaxation scattering rate. The inter-band contribution σ_I contains the characteristic function $G(u) = \sinh(u/k_B T)/[\cosh(\mu/k_B T) + \cosh(u/k_B T)]$.

The spectral function for the TM polarization experiences a maximum around the graphene plasmon frequency $\hbar\omega^p_{max} \sim \hbar\omega^{pr}_p(q) \approx \sqrt{e^2 k_B T q \ln\left[2\cosh\left(\mu/2k_B T\right)\right]}$,[17] which is obtained by using the dominant intra-band component of the conductivity and equating to zero the reflection coefficient $-\rho_{p1,2} = 0$. Therefore, the dependence of the graphene plasmon frequency on μ and q allow for tunability of the TM NF radiation with different materials.[7]

In typical plasmonic materials the TE mode channel is ineffective for NF heat transfer, because it does not allow for surface plasmons. In graphene, however, the TE surface plasmon exists.[12] This stems from the Dirac like energy dispersion and the subsequent interplay between the imaginary parts of the inter-band and intra-band conductivity. The TE contribution to the NF heat has been ignored by other researchers as being small compared to the TM modes.[7,18] In this paper, we aim at finding ways to enhance the s-polarization by first providing a fundamental description of this contribution to the radiation process. This knowledge is then utilized for designing a scheme capable of further control and enhancement of the radiative exchange.

The non-transparent expression for $f_s^{NF}(\omega)$ from Equation (1) can be recast in a simpler, analytical form by noticing that the largest contribution to the power, *P*, happens when $q >> \omega / c$. This means that the TE plasmon excitations is very close to the photon line and the intra-band σ_D is almost entirely responsible for the TE NF radiation. This enables finding an approximate expression (details in the Supporting Information) for $\mu >> k_B T$,

$$f_s^{NF} \approx -\left(\frac{2\omega\alpha\mu\Gamma}{\pi\hbar c(\omega^2+\Gamma^2)}\right)^2 \times \left[1.44764 + \ln\left(\frac{4\sqrt{6}d\alpha\mu}{\hbar c}\frac{\omega^2}{\omega^2+\Gamma^2}\right)\right], \quad (3)$$

where α is the fine structure constant. Using Equation (3), one further finds that $f_s^{NF}(\omega)$ experiences a resonant maximum at

$$\omega^s_{max} \approx \Gamma. \quad (4)$$

The results from Equations (3) and (4) are quite interesting. They show that the carrier scattering processes captured in Γ play a decisive role for the TE contribution in the NF heat exchange. The location of the maximum scales linearly with Γ, but the strength of $f_s^{NF} \propto \mu^2$, and it is weakly (logarithmic) dependent on the distance. Our numerical calculations using Equations (1) and (2) are shown in **Figure 1**a, and they are in precise agreement with the analytical expressions in Equations (3) and (4).

The behavior for the p-polarized spectral function is quite different as compared to f_s^{NF}. The position of the TM resonant maximum is controlled by the chemical potential and the magnitude of f_p^{NF} is Γ dependent, as can be seen in Figure 1b. Comparing Figure 1a and b, it appears that the roles that μ and Γ play for the two NF channels are reversed. Changing μ shifts the TM resonance, while it only changes the magnitude of the spectral function for the TE contribution. On the other hand, Γ is responsible for the location of the TE resonance, yet it is important for the magnitude of the TM contribution.

The interaction between graphene and a metamaterial is now considered. The manipulation "knobs", μ and Γ, show that there are previously unexplored ways to control the heat exchange. It has been suggested in previous works,[7,18] that the chemical potential of graphene is an effective way to modulate NF heat exchange, where the TE contribution was neglected as being small. However, by shifting the TM resonance to higher frequencies, by increasing μ, and by pining the TE resonance in the infrared range, one can obtain a stronger s-polarized NF heat exchange. We note that μ can be modulated by external fields, carrier concentration or by chemical doping, and Γ is sensitive to the carrier concentration and scattering mechanisms taking place in the system.[19,20] We further suggest that the

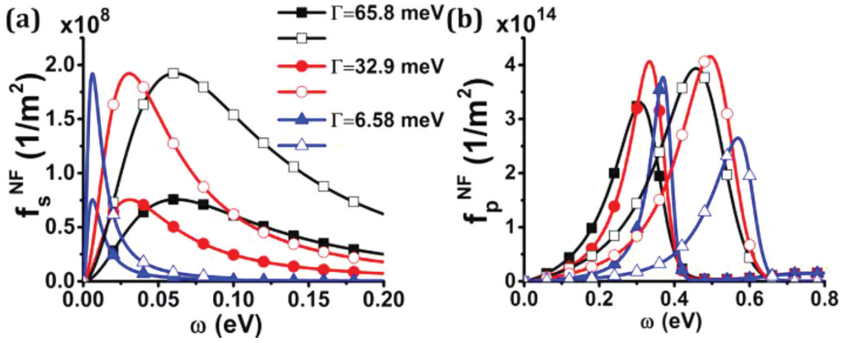

Figure 1. Spectral function as a function of frequency at $T = 300$ K for: (a) s-polarized modes; (b) p-polarized modes. Three different scattering rates are shown. The solid symbols correspond to $\mu = 0.3$ eV and the open symbols to $\mu = 0.5$ eV.

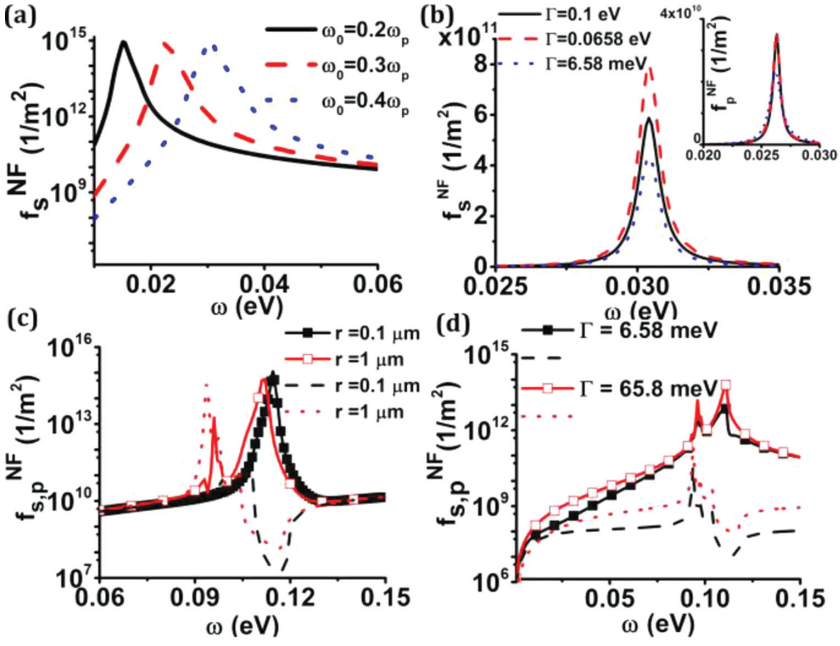

Figure 2. Spectral functions vs frequency ω for the (a) TE contribution between two Pendry-like MMs for different ω_0; (b) TE contribution between suspended graphene and Pendry-like MM substrate with $\mu = 0.5$ eV, $\omega_0 = 0.4\ \omega_p$, $n = 1.5$, $T = 300$ K for different graphene scattering rates. The insert shows the TM contribution; (c) TE and TM contributions between two SiC sphere based MMs for different sphere radii. The dashed and dotted graphs represent the TE mode and the connected graphs the TM mode; (d) TE and TM contributions between graphene and SiC based MM for two graphene scattering rates and sphere radius $r = 1\,\mu$m. Typical parameters for the Pendry-like material are $\omega_p = 0.0658$ eV, $\Gamma_m = 0.01\omega_p$, and $F = 0.5$.[9] Typical parameters for the SiC are $\omega_{TO} = 0.0983$ eV, $\omega_{LO} = 0.12$ eV, $\varepsilon_\infty = 6.7$, $\Gamma_{SiC} = 0.00059$ eV.[26] The KBr matrix has $n = 1.5$. The separation in all cases is $d = 10$ nm.

preferentially polarized NF radiation can be utilized to detect graphene TE excitations and can be used as a tool to measure its scattering rates and their temperature dependence.

In order to further modulate the TE and TM heat exchange channels, one can utilize graphene/MM systems. Optical MMs are composed of a suitable combination of dielectric and metallic components, which can be described in terms of circuit elements building units. Because of the strong dielectric and magnetic responses, many novel effects have been observed. Negative index of refraction, reversed Doppler shift, superlenses, and optical cloaks have been reported by utilizing MMs.[13]

Here we consider a half-space MM substrate (1) and a free standing graphene sheet (2) separated by a distance d. The reflection coefficients for the MM-free space interface are

$$\rho_{p1} = \frac{\varepsilon_m h_0 - h}{\varepsilon_m h_0 + h}, \rho_{s1} = \frac{\mu_m h_0 - h}{\mu_m h_0 + h}, \quad (5)$$

where $h_0 = \sqrt{q^2 - \omega^2/c^2}$ and $h = \sqrt{q^2 - \varepsilon_m \mu_m \omega^2/c^2}$. ε_m and μ_m are the MM permittivity and permeability, respectively. The graphene coefficients $\rho_{s,p2}$ were specified in Section 3. Equation (5) shows that the s-polarization contribution to the radiation is directly related to the magnetic response μ_m of the MM, which couples with the graphene TE excitations. The p-polarization contribution is mainly determined by its dielectric response ε_m, which couples to the graphene TM modes. For enhanced TE and/or TM NF exchange to occur, resonant coupling between the relevant modes must be achieved in the infrared range due to the overlap in the infrared with temperature function $\Theta(\omega)$ as already discussed.

We assume that the MM substrate can be described via an effective medium theory, which is suitable when the size of the MM unit cell is much smaller than the wavelength of the electromagnetic radiation $\lambda \sim 10\,\mu$m. In this case, the magnetic response μ_m of many MMs, such as split ring resonators and split wire or rod pairs, is given by $\mu_m = 1 - \frac{F\omega^2}{\omega^2 - \omega_0^2 + i\omega\Gamma_m}$, where F is the volume fraction of the resonator that allows for a magnetic response.[21,22] The effective magnetic resonance occurs at ω_0, usually in the infrared range, with characteristic losses described by Γ_m.[15,23] For MMs composed of disconnected unit components, such as wires or rods, the effective dielectric response ε_m may be describes by a Lorentz oscillator whose response occurs in the optical regime,[24,25] thus the Drude term is not present in ε_m. We note that in this case, it suffices to take $\varepsilon_m = n^2$, where n is the index of refraction, as the high frequency resonances are not important due to the small overlap with the Θ-function from Equation (1).

Figure 2a shows the NF s-polarized spectral function between two identical MMs as specified above. Using Equations (5) and (6), we find that f_s^{NF} has a resonant maximum at $\omega_s = \sqrt{2}\omega_0 / \sqrt{2 - F}$, which is found by equating the denominator of its reflection coefficient ρ_{s1} to zero. Typically, the filling factor for Pendry-like MMs is $F \sim 0.1 - 0.5$,[27] and ω_0 may be in the infrared.[13] Also, due to the large resonant optical frequencies in the dielectric response ($\varepsilon_m = n^2$ for the disconnected MMs), the TM contribution is several orders of magnitude smaller than the TE one, thus it is not displayed.

The NF radiation between a suspended graphene sheet and a MM substrate is also considered. Figure 2b shows that a strong coupling between the s-polarized modes from the graphene and the MM can be achieved. The location of the f_s^{NF} maximum is determined by ω_s mainly via ω_0. The magnitude of the spectral function, however, is strongly dependent upon the graphene scattering rate Γ. At the same time, the p–polarization is not significantly affected by Γ, and it is strongly suppressed, at least by an order of magnitude as compared to f_s^{NF}. The location of the f_p maximum is around ω_0. The MM losses also play a secondary effect, as larger Γ_m somewhat reduce the magnitude of the f_s peak and make it broader, while smaller values of Γ_m have an opposite effect. The broadening of f_s mildly increases the radiative heat transfer.

In addition to the Pendry type systems, MMs composed entirely of dielectric components can be constructed. Recent reports show that it is possible to obtain a strong dielectric

and magnetic response in the infrared from a substrate, which consists of a KBr host with an inclusion of a large number of SiC spheres.[28] Using the Mie scattering approach within the Clausius-Mossotti approximation, the permittivity and permeability for such materials have been derived.[26] These effective medium results are valid when the electromagnetic wavelength is much larger than the radius of the sphere *r*, which is the case here.

We explore how the NF heat transfer with graphene can be modulated by using a KBr/SiC dielectric type of MM instead of the Pendry-like system discussed previously. We use the effective permittivity and permeability model via the Mie scattering theory (details of the model are described in Ref.[26], which requires the dielectric response for SiC, $\varepsilon_{SiC}(\omega)=\varepsilon_{\infty}\left(1-\frac{\omega_{TO}^2-\omega_{LO}^2}{\omega^2-\omega_{TO}^2+i\Gamma_{SiC}}\right)$, where ω_{TO} is the transverse optical phonon frequency, ω_{LO} is the longitudinal optical phonon frequency, Γ_{SiC} is the scattering rate for SiC,and ε_{∞} is the optical dielectric constant. $\varepsilon_{SiC}(\omega)$ contains the characteristics for SiC surface phonon-polaritons in the infrared, which is a key property for radiative enhancement.

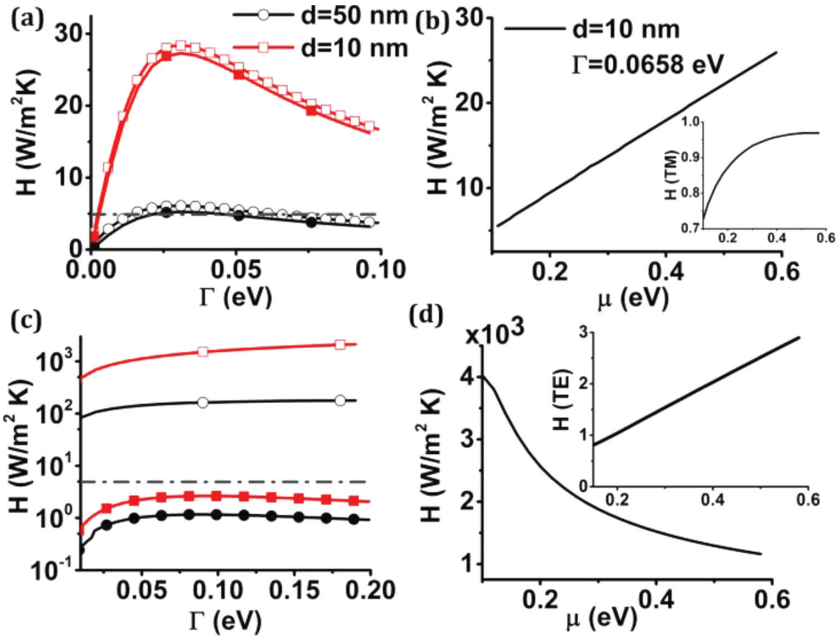

Figure 3. NF heat transfer coefficient between: (a) a Pendry MM and graphene vs Γ for two separations *d* at $T = 300$ K. Open symbols – net heat transfer; solid symbols – TE contribution, μ = 0.5 eV; (b) Pendry MM and graphene vs μ. The inset shows the TM mode contribution. (c) graphene and dielectric MM vs Γ. Open symbols – net heat coefficient; solid symbols – TE contribution. The radius of SiC spheres is 1 μm; (d) graphene and dielectric MM vs μ. The insert shows the TE contribution. The dash-dotted line in a) and c) shows the FF contribution $H \approx 4.9$ W/m²K.

Figure (2c) shows the spectral decomposition of the NF radiation between two dielectric MMs composed of larger and smaller SiC spheres. The effect of the spheres' radius on f_s^{NF} is more pronounced as compared to the f_p^{NF} function. The TE contribution varies by several orders of magnitude as the resonant peak is stronger for the larger spheres. Nevertheless, the TM contribution is always stronger. Figure 2d shows the spectral distribution when one of the substrates is replaced by graphene. The graphene scattering rate Γ affects f_s^{NF} in a more profound way as compared to f_p^{NF}. The radiation, however, is dominated by the TM modes as displayed in Figure 2d.

To further investigate the heat transfer in the graphene/MM systems, the heat transfer coefficient *H* is considered,

$$H=\lim_{\Delta T\to 0}\frac{P(T,T+\Delta T)}{\Delta T}, \quad (6)$$

where *P* is the total radiative intensity transferred, obtained via Equation (1). *H* characterizes the overall heat exchange process per a small change in temperature. Here we calculate this quantity to give an expanded perspective of how the heat exchange can be controlled using the graphene sheet properties.

Figure 3a and b show the dependence of the graphene relaxation rate and chemical potential on the heat transfer between graphene and a Pendry-like MM. It is clear that the NF radiation is dominated by the s-polarization, which experiences a maximum as a function of Γ. For comparison, the FF transfer coefficient is also shown. It turns out that the far-field is mostly independent of distance. On the other hand, the near-field *H* quickly decreases as the separation is increased, and at $d = 50$ *nm* the near-field and far-field contribute about the same. The dependence of *H* upon *μ* is linear (Figure 3b), which reflects the dominant TE heat transfer whose magnitude is $\propto\mu$. The contribution from the TM modes vs *μ* is nonlinear and greatly reduced, as the insert shows.

For the SiC based MM/graphene system, the heat transfer coefficient can be enhanced significantly as Γ is increased, as shown in Figure 3c. The process is completely dominated by the p-polarization, while the TE contribution is eclipsed by the FF heat transfer. Also, *H* decreases in a non-linear fashion vs *μ* mainly due to the TM polarization (Figure 3d). The decrease can be explained by the fact that the graphene surface plasmons are excited at higher frequency for larger *μ*.

By exploring the electromagnetic interaction between suspended graphene and artificial materials, interesting possibilities are revealed. Graphene supports surface plasmon modes with TE and TM polarizations, but in most processes the TM modes are dominant. Our results show that by using properly constructed optical MMs, it is possible to enhance the elusive s-polarized graphene excitations through a coupling to the MM s-polarized modes via near-field radiation exchange.

This indicates not only a way to control heat transfer for suspended graphene sheets, but it also reveals a way to measure certain physical graphene characteristics, which may not be attainable by other methods. Specifically, we showed that for Pendry-like MM substrates, the radiation may be dominated by the s-polarization, which gives an excellent way to measure the infrared relaxation scattering time of suspended graphene.

Experimental techniques relying on ultrafast pump-probe spectroscopy, Josephson's junctions supercurrents, or magnetoresistance meausrements have been reported.[29–31] However, such techniques are used for graphene sheets deposited on various substrates. Here we propose that near-field heat transfer can be a viable tool to measure the scattering time for a suspended graphene above a MM. In addition, existing techniques are usually applicable for a particular temperature. Here, by varying T it may be possible to obtain a temperature profile of the graphene scattering time. This in turn can serve to probe different scattering mechanisms since theoretical studies have shown that Γ is influenced by a particular scattering process at a given temperature range.[19]

Another important functionality is that enhanced near-field heat transfer is possible between two dissimilar materials if graphene is used. The strong dependence on the chemical potential enables enhancing the magnitude of the process as well by shifting the frequency dependence in resonance with the properties of the substrate. This can be done by changing μ via external fields or dopant concentration, for example. Note that for typical systems, the resonant coupling occurs for two materials that are the same, contrary to the case studied here.

In conclusion, near-field radiation involving graphene sheets and optical MMs was studied. Our calculations show that this is a viable way to detect the graphene TE modes by utilizing artifial MMs as substrates. The heat exchange process can also be used as a tool to characterize the graphene carrier scattering rate and chemical potential and their interrelation. This work reveals ideas for further control of near-field heat transfer involving graphene and artificial composite materials.

Supporting Information

Supporting Information is available from the Wiley Online Library or from the author.

Acknowledgements

We acknowledge financial support from the Department of Energy under contract DE-FG02-06ER46297. Discussions with Prof. Jiangfeng Zhou and Dr. Diego Dalvit are also acknowledged.

Received: June 13, 2014
Revised: July 16, 2014
Published online: August 28, 2014

[1] H. B. G. Casimir, *Proc. K. Ned. Akad. Wet.* **1948**, *51*, 793.
[2] M. S. Tomassone, A. Widom, *Phys. Rev. B* **1997**, *56*, 4938.
[3] D. Polder, M. Van Hove, *Phys. Rev. B* **1971**, *4*, 3303.
[4] S. Basu, Z. M. Zheng, C. J. Fu, *Int. J. En. Res.* **2009**, *33*, 1203.
[5] P. Ben-Abdallah, K. Joulain, *Phys. Rev. B* **2010**, *82*, 121419R.
[6] A. Murray, W. L. Barnes, *Adv. Mater.* **2007**, *19*, 3771.
[7] V. B. Svetovoy, P. J. van Zwol, J. Chevrier, *Phys. Rev. B* **2012**, *85*, 155418.
[8] P. J. van Zwol, S. T. C. Berger, W. A. de Heer, J. Chevrier, *Phys. Rev. Lett.* **2012**, *109*, 264301.
[9] A. Passian, A. Wig, L. Lereu, F. Meriaudeau, T. Thundat, T. L. Ferrell, *Appl. Phys. Lett.* **2004**, *85*, 3420.
[10] S. Shen, A. Narayanaswamy, G. Chen, *Nano Lett.* **2009**, *9*, 2909.
[11] R. S. Ottens, V. Quetschke, S. Wise, A. A. Alemi, R. Lundock, G. Mueller, D. H. Reitze, D. B. Tanner, B. F. Whiting, *Phys. Rev. Lett.* **2011**, *107*, 014301.
[12] a) S. A. Mikhailov, K. Ziegler, *Phys. Rev. Lett.* **2007**, *99*, 016803; b) M. Bordag, I. G. Pirozhenko, *Phys. Rev. B* **2014**, *89*, 035421.
[13] C. M. Soukoulis, M. Wegener, *Nature Photonics* **2011**, *5*, 523.
[14] A. Vakil, N. Engheta, *Science* **2011**, *332*, 1291.
[15] K. Joulain, J. Drevillon, P. Ben-Abdallah, *Phys. Rev. B* **2010**, *81*, 165119.
[16] L. A. Falkovsky, A. A. Varlamov, *Eur. Phys. J. B* **2010**, *56*, 281.
[17] O. Vafek, *Phys. Rev. Lett.* **2006**, *97*, 266406.
[18] O. Ilic, M. Jablan, J. D. Joannopoulos, I. Celanovic, H. Buljan, M. Soljacic, *Phys. Rev. B* **2012**, *85*, 155422.
[19] a) E. H. Hwang, S. Das Sarma, *Phys. Rev. B* **2008**, *77*, 195412; b) T. Stauber, N. M. R. Peres, F. Guinea, *Phys. Rev. B* **2007**, *76*, 205423.
[20] K. F. Mak, F. H. Da Hornada, K. He, J. Deslippe, N. Petrone, J. Hone, J. Shan, S. G. Louie, T. F. Heinz, *Phys. Rev. Lett.* **2014**, *112*, 207401.
[21] J. B. Pendry, A. J. Holden, D. J. Robbins, W. J. Stewart, *IEEE Trans. Microwave Theory Techniques* **1999**, *47*, 2075.
[22] D. R. Smith, W. J. Padilla, D. C. Vier, S. C. Nemat-Nasser, S. Schultz, *Phys. Rev. Lett.* **2000**, *84*, 4184.
[23] Z. Zheng, Y. Xuan, *Int. J. Heat Mass Transfer* **2011**, *54*, 1101.
[24] D. B. Tanner, A. J. Sievers, R. A. Buhrman, *Phys. Rev. B* **1975**, *11*, 1330.
[25] J. B. Pendry, A. J. Holden, D. J. Robbins, W. J. Stewart, *J. Condens. Matter* **1998**, *10*, 4785.
[26] M. Francoeur, S. Basu, S. J. Petersen, *Opt. Exps.* **2011**, *19*, 18774.
[27] P. Tassin, T. Koschny, M. Kafesaki, C. M. Soukoulis, *Nat. Photonics* **2012**, *6*, 259.
[28] S. J. Petersen, S. Basu, B. Raeymaekers, M. Francoeur, *J. Quantitative Spectroscopy Radiative Transfer* **2013**, *129*, 277.
[29] J. M. Dawlaty, S. Shivaraman, M. Chandrashekhar, F. Rana, M. G. Spencer, *Appl. Phys. Lett.* **2008**, *92*, 042116.
[30] J. Voutilainen, A. Fay, J. K. Viljas, T. T. Heikkila, P. J. Hakonen, *Phys. Rev. B* **2011**, *84*, 045419.
[31] M. Monteverde, C. Ojeda-Aristizabal, R. Weil, K. Bennaceur, M. Ferrier, S. Geuron, C. Glattli, H. Bouchiat, J. N. Fuchs, D. L. Maslov, *Phys. Rev. Lett.* **2010**, *104*, 126801.